Contribution of the spin-1 diquark to the nucleon's g_1 structure function

F. Zamani
Department of Physics, Villanova University, Villanova, Pennsylvania 19085, USA
(Received 13 April 2010; published 19 July 2010)

This is the final installment of a series of work that we have done in the context of the meson cloud model that investigates F_2 and g_1 structure functions. In our previous work on g_1 structure function, we showed that having a spin-0 quark-diquark for the nucleon core along with both pseudoscalar and vector meson clouds was not sufficient to reproduce experimental observation(s) consistently. For the F_2 structure function, we found that both superposition of a spin-0 diquark and a spin-1 diquark in the nucleon core along with pseudoscalar and vector meson clouds are needed to reproduce the observed $F_2(x)$ and the Gottfried sum rule (GSR) violation. Therefore, in the present work, we consider the contribution of a spin-1 diquark in the nucleon core to the g_1 structure function. The calculation is performed in the light-cone frame. The dressed nucleon is assumed to be a superposition of the bare nucleon plus virtual light-cone Fock states of baryon-meson pairs. For the bare nucleon, we consider different quark-diquark configurations along with the possibility that there is no diquark inside the nucleon. The initial distributions are evolved. The final results are compared with experimental results and other theoretical predictions.

DOI: 10.1103/PhysRevC.82.015204 PACS number(s): 12.39.Ki, 14.20.Dh, 14.65.Bt, 24.85.+p

I. INTRODUCTION

The meson cloud model (MCM) has been used extensively for both polarized and unpolarized nucleon structures. It all started with Sullivan's original work in 1972 [1], which pointed out the significance of the pionic structure of the nucleon in high-energy processes. Sullivan examined the role of the one-pion exchange in deep inelastic scattering from nucleons. Being the lightest meson, the pion is expected to play a dominant role in the nucleon structure. However, this does not exclude the contribution of other mesons to the nucleon structure. Therefore, the mesonic structure of the nucleon, or the so-called the meson cloud, can have contributions not only from the pion but from other members of the pseudoscalar and vector mesons octets. Since the 1990s, both unpolarized [2,4–6,8–30] and polarized [31–39] nucleon structures have been investigated using the MCM.

Since late 1980s, there has been a flurry of activity investigating the spin structure of the nucleon. Measurements by the European Muon Collaboration (EMC) started it all by indicating that only a small fraction of the proton spin is carried by the spin of the quarks [40,41]. Because this was in disagreement with the quark model predictions, a model that had great success in describing the gross features of the nucleon, the EMC result caused quite a stir in the particle physics community. This resulted in the "proton spin crisis" and a considerable amount of both theoretical and experimental investigations of the nucleon spin. Since then, literally hundreds of papers have been published on this subject. On the experimental side, the original experiment by EMC at CERN was followed by experiments conducted by the Spin Muon Collaboration (SMC) [42–50], the Stanford Linear Accelerator Center (SLAC) [51–62], the HERMES collaboration at Deutsches Elektronen-Synchrotron (DESY) [63–66], and the Jefferson Lab [67–72]. Among other things, these experiments have confirmed the original EMC result, the Bjorken sum rule (BSR) [73,74] but have shown the violation of the Ellis-Jaffe sum rule (EJSR) [75] and what appears to be a large negative strange quark polarization.

The objective of the theoretical work is to find the contribution of different sources, that is, quarks, gluons, and orbital motion of the partons, to the spin of the proton. In the late 1980s, Altarelli and Ross [76] and Carlitz, Collins, and Mueller [77] suggested that there is a hard gluonic contribution to the first moment of the g_1 structure function of the proton. Others followed up on this suggestion [78–80]. The objective was to see whether a positive gluon polarization exists, since this would explain the large negative sea polarization and the rather small contribution of the quarks to the spin of the proton. For a period of time, there was some apparent conflict between the chiral invariant approach and the gauge invariant approach to the calculation of the contribution of the gluon to the quark polarization, because in the operator product expansion approach, which is model independent, the hard gluons at the twist-2 level make no contribution to the first moment of g_1 structure function. This apparent problem has been clarified [79,81], and one can consider the possibility of contribution as a result of gluon anomaly, which is not unexpected in a perturbative QCD (pQCD) regime [82]. Although recent experimental evidence points to small gluon polarization, the uncertainty in the shape of the gluon distribution is large enough that excluding high gluon polarization is not possible [83–86]. Therefore, by considering the observed experimental results as superpositions of the quark and gluon polarizations, one can resolve the spin crises. For interested readers, there are a number of excellent extended articles on this topic [86–99].

In Sec. II, we briefly present a light-front representation of three-body systems and introduce the two types of wave functions that we use for the nucleon core. This is followed by the formalism for the MCM in Sec. III. Results and discussion are presented in Sec. IV, which is followed by a summary in Sec. V.

II. LIGHT-FRONT REPRESENTATION OF THE NUCLEON

Since the original work by Dirac [100] several decades ago, there has been extensive use of the light-front frame to study high-energy processes [101–104]. Basic definitions and formalism are discussed in Refs. [105,106]. A four-vector in the light-front frame is defined as

$$a = (a^+, a_-, a_\perp), \tag{1}$$

where $a^\pm = (a^\circ \pm a^3)/\sqrt{2}$ and $a_\perp = (a^1, a^2)$. Following the relativistic treatment of the nucleon by Berestetskii and Terent'ev [107,108], we separate the center-of-mass motion of the three quarks in the nucleon from their relative motion by transforming their momenta, p_1, p_2, p_3, into total and relative momenta as follows:

$$\vec{P} = \vec{p}_1 + \vec{p}_2 + \vec{p}_3, \tag{2a}$$

$$\xi = \frac{p_1^+}{p_1^+ + p_2^+}, \quad \eta = \frac{p_1^+ + p_2^+}{P^+}, \tag{2b}$$

$$q_\perp = (1-\xi)p_{1\perp} - \xi p_{2\perp},$$

$$Q_\perp = (1-\eta)(p_{1\perp} + p_{2\perp}) - \eta p_{3\perp}. \tag{2c}$$

Then, the Hamiltonian of the system takes the form

$$H = \frac{P_\perp^2 + \hat{M}^2}{2P^+}, \tag{3}$$

where $\hat{M}$ is the mass operator with the interaction term W:

$$\hat{M} = M + W, \tag{4a}$$

$$M^2 = \frac{Q_\perp^2}{\eta(1-\eta)} + \frac{M_3^2}{\eta} + \frac{m_3^2}{1-\eta}, \tag{4b}$$

$$M_3^2 = \frac{q_\perp^2}{\xi(1-\xi)} + \frac{m_1^2}{\xi} + \frac{m_3^2}{1-\xi}, \tag{4c}$$

with m_1, m_2, and m_3 as the constituent quarks masses. M and M_3 can be rewritten in a more transparent way in terms of the relative momenta q and Q:

$$E_1 = \sqrt{\mathbf{q}^2 + m_1^2}, \quad E_2 = \sqrt{\mathbf{q}^2 + m_2^2},$$
$$E_3 = \sqrt{\mathbf{Q}^2 + m_3^2}, \quad E_{12} = \sqrt{\mathbf{Q}^2 + M_3^2}, \tag{5a}$$

$$\xi = \frac{E_1 + q_3}{E_1 + E_2}, \quad \eta = \frac{E_{12} + Q_3}{E_{12} + E_3}, \tag{5b}$$

$$M = E_{12} + E_3, \quad M_3 = E_1 + E_2, \tag{5c}$$

where $\mathbf{q} = (q_1, q_2, q_3)$ and $\mathbf{Q} = (Q_1, Q_2, Q_3)$.

The wave function of the nucleon can be written as

$$\Psi = \Phi\chi\phi, \tag{6}$$

where Φ, χ, and ϕ are the flavor, spin, and momentum distributions, respectively. We are going to consider two different wavefunctions for the core nucleon. First, assume that the nucleon is a quark-diquark system. In general, the nucleon state can be a linear combination of the following spin-isospin diquark states: (0,0), (0,1), (1,0), and (1,1) written as:

$$\Psi_1 = \frac{A}{\sqrt{2}}\big[uud\big(\chi^{\rho 1}\phi_1^{\lambda 1} + \chi^{\rho 2}\phi_1^{\lambda 2}\big) - udu\big(\chi^{\rho 1}\phi_1^{\lambda 1} - \chi^{\rho 3}\phi_1^{\lambda 3}\big) - duu\big(\chi^{\rho 2}\phi_1^{\lambda 2} + \chi^{\rho 3}\phi_1^{\lambda 3}\big)\big]$$
$$+ \frac{B}{\sqrt{6}}\big[uud\big(\chi^{\rho 1}\phi_1^{\rho 1} + \chi^{\rho 2}\phi_1^{\rho 2} - 2\chi^{\rho 3}\phi_1^{\rho 3}\big) + udu\big(\chi^{\rho 1}\phi_1^{\rho 1} - 2\chi^{\rho 2}\phi_1^{\rho 2} + \chi^{\rho 3}\phi_1^{\rho 3}\big) + duu\big(-2\chi^{\rho 1}\phi_1^{\rho 1} + \chi^{\rho 2}\phi_1^{\rho 2} + \chi^{\rho 3}\phi_1^{\rho 3}\big)\big]$$
$$+ \frac{C}{\sqrt{2}}\big[uud\big(\chi^{\lambda 1}\phi_1^{\rho 1} + \chi^{\lambda 2}\phi_1^{\rho 2}\big) - udu\big(\chi^{\lambda 1}\phi_1^{\rho 1} - \chi^{\lambda 3}\phi_1^{\rho 3}\big) - duu\big(\chi^{\lambda 2}\phi_1^{\rho 2} + \chi^{\lambda 3}\phi_1^{\rho 3}\big)\big]$$
$$+ \frac{D}{\sqrt{6}}\big[uud\big(\chi^{\lambda 1}\phi_1^{\lambda 1} + \chi^{\lambda 2}\phi_1^{\lambda 2} - 2\chi^{\lambda 3}\phi_1^{\lambda 3}\big) + udu\big(\chi^{\lambda 1}\phi_1^{\lambda 1} - 2\chi^{\lambda 2}\phi_1^{\lambda 2} + \chi^{\lambda 3}\phi_1^{\lambda 3}\big) + duu\big(-2\chi^{\lambda 1}\phi_1^{\lambda 1} + \chi^{\lambda 2}\phi_1^{\lambda 2} + \chi^{\lambda 3}\phi_1^{\lambda 3}\big)\big]. \tag{7a}$$

For the second case we assume that there is no cluster of quarks inside the nucleon [105,106]:

$$\Psi_2 = \frac{-1}{\sqrt{3}}(uud\chi^{\lambda 3} + udu\chi^{\lambda 2} + duu\chi^{\lambda 1})\phi_2. \tag{7b}$$

We will be using three wavefunctions called set 1, set 2 and set 3. Set 1 and set 2 correspond to the models that we have used in Refs. [31,32]. Set 1 is the spin-0 diquark with $A = .9798$, $B = -.2$, $C = 0.0$ and $D = 0.0$ in Eq. (7a). Set 2 is Eq. (7b). Set 3 is the new model in which we choose $A = -0.7874$, $B = 0.0$, $C = 0.0$, and $D = -0.6164$ in Eq. (7a). Also, in Eq. (7), u and d represent the up and down flavor, and χ^{ρ_i} and χ^{λ_i} with $i = 1, 2, 3$ represent the Melosh transformed spin wave functions [109]. For example,

$$\chi_\uparrow^{\rho 3} = \frac{1}{\sqrt{2}}(\uparrow\downarrow\uparrow - \downarrow\uparrow\uparrow), \tag{8a}$$

$$\chi_\downarrow^{\rho 3} = \frac{1}{\sqrt{2}}(\uparrow\downarrow\downarrow - \downarrow\uparrow\downarrow), \tag{8b}$$

$$\chi_\uparrow^{\lambda 3} = \frac{1}{\sqrt{6}}(\downarrow\uparrow\uparrow + \uparrow\downarrow\uparrow - 2\uparrow\uparrow\downarrow), \tag{8c}$$

$$\chi_\downarrow^{\lambda 3} = \frac{1}{\sqrt{6}}(2\downarrow\downarrow\uparrow - \downarrow\uparrow\downarrow - \uparrow\downarrow\downarrow). \tag{8d}$$

The spin wave function of the ith quark is

$$\uparrow = R_i \begin{pmatrix} 1 \\ 0 \end{pmatrix}, \quad \downarrow = R_i \begin{pmatrix} 0 \\ 1 \end{pmatrix}. \tag{9}$$

In Eq. (9), R_i are the Melosh matrices:

$$R_1 = \frac{1}{\sqrt{a^2 + Q_\perp^2}\sqrt{c^2 + q_\perp^2}} \begin{pmatrix} ac - q_R Q_L & -aq_L - cQ_L \\ cQ_R + aq_R & ac - q_L Q_R \end{pmatrix}, \tag{10a}$$

$$R_2 = \frac{1}{\sqrt{a^2 + Q_\perp^2}\sqrt{d^2 + q_\perp^2}} \begin{pmatrix} ad + q_R Q_L & -aq_L - dQ_L \\ dQ_R - aq_R & ad - q_L Q_R \end{pmatrix},$$

$$R_3 = \frac{1}{\sqrt{b^2 + Q_\perp^2}} \begin{pmatrix} b & Q_L \\ -Q_R & b \end{pmatrix}, \tag{10b}$$

where

$$a = M_3 + \eta M, \quad b = m_3 + (1-\eta)M, \tag{11a}$$

$$c = m_1 + \xi M_3, \quad d = m_2 + (1-\xi)M_3, \tag{11b}$$

$$q_R = q_1 + iq_2, \quad q_L = q_1 - iq_2, \tag{11c}$$
$$Q_R = Q_1 + iQ_2, \quad Q_L = Q_1 - iQ_2. \tag{11d}$$

The functions $\phi_1^{\rho i}$ and $\phi_1^{\lambda i}$, with $i = 1, 2, 3$, and ϕ_2, are the momentum wave functions, which we take be of the following form:

$$\phi_1^{\rho i} = N_{\rho i}(X_j - X_k)\phi_1^{si}/X_T, \tag{12a}$$
$$\phi_1^{\lambda i} = N_{\lambda i}(X_j + X_k - 2X_i)\phi_1^{si}/X_T, \tag{12b}$$

with $i \neq j \neq k$, and [105]

$$\phi_2 = \frac{N}{(M^2 + \beta^2)^{3.5}}. \tag{12c}$$

Also,

$$X_3 = \frac{Q_\perp^2}{2\eta(1-\eta)\beta_Q^2} + \frac{q_\perp^2}{2\eta\xi(1-\xi)\beta_q^2} + \frac{m_1^2}{2\eta\xi\beta_q^2} + \frac{m_2^2}{2\eta(1-\xi)\beta_q^2} + \frac{m_3^2}{2(1-\eta)\beta_Q^2}, \tag{13a}$$

$$X_2 = q_\perp^2 \frac{(1-\eta)(1-\xi)\beta_Q^2 + \xi\beta_q^2}{2\beta_Q^2\beta_q^2\eta\xi(1-\xi)(1-\eta+\xi\eta)} + Q_\perp^2 \frac{(1-\xi)(1-\eta)\beta_q^2 + \xi\beta_Q^2}{2\beta_Q^2\beta_q^2\eta(1-\eta)(1-\eta+\xi\eta)} + q_\perp Q_\perp \frac{\beta_Q^2 - \beta_q^2}{\beta_Q^2\beta_q^2\eta(1-\eta+\xi\eta)} + \frac{m_1^2}{2\eta\xi\beta_q^2} + \frac{m_2^2}{2\eta(1-\xi)\beta_Q^2} + \frac{m_3^2}{2(1-\eta)\beta_q^2}, \tag{13b}$$

$$X_1 = q_\perp^2 \frac{(1-\xi)\beta_q^2 + \xi(1-\eta)\beta_Q^2}{2\beta_Q^2\beta_q^2\eta\xi(1-\xi)(1-\xi\eta)} + Q_\perp^2 \frac{(1-\xi)\beta_Q^2 + \xi(1-\eta)\beta_q^2}{2\beta_Q^2\beta_q^2\eta(1-\xi)(1-\xi\eta)} - q_\perp Q_\perp \frac{\beta_Q^2 - \beta_q^2}{\beta_Q^2\beta_q^2\eta(1-\xi\eta)} + \frac{m_1^2}{2\eta\xi\beta_Q^2} + \frac{m_2^2}{2\eta(1-\xi)\beta_q^2} + \frac{m_3^2}{2(1-\eta)\beta_q^2}, \tag{13c}$$

$$X_T = X_1 + X_2 + X_3, \tag{13d}$$

and

$$\phi_1^{si} = \frac{1}{(1+X_T)^{ni}}. \tag{13e}$$

In these equations, β_Q, β_q, and β are confinement scale parameters and N_{ρ_i}, N_{λ_i}, and N are normalization constants.

III. MESON CLOUD MODEL IN LIGHT-CONE FRAME

The MCM has been used extensively in the 1990s, mostly to investigate the flavor asymmetry of the nucleon sea. In this approach using the convolution model, one can decompose the physical nucleon in terms of the nucleon core and intermediate, virtual meson-baryon states [1,2,4–39]. Following the work done by Zoller [14], Holtmann, Szczurek, and Speth [36], and Speth and Thomas [37], one can write

$$|N\uparrow\rangle = Z^{1/2}\Bigg[|N\uparrow\rangle_{\text{bare}} + \sum_{BM}\sum_{\lambda\lambda'}\int dy d^2k_\perp \beta_{BM}^{\lambda\lambda'}(y, k_\perp^2) \times |B^\lambda(y, \vec{k}_\perp); M^{\lambda'}(1-y, -\vec{k}_\perp)\rangle\Bigg], \tag{14a}$$

with

$$\beta_{BM}^{\lambda\lambda'}(y, k_\perp^2) = \frac{1}{2\pi\sqrt{y(1-y)}} \frac{\sqrt{m_N m_B} V_{IMF}^{\lambda\lambda'}(y, k_\perp^2)}{m_N^2 - M_{BM}^2(y, k_\perp^2)}, \tag{14b}$$

where Z is the probability of the physical nucleon being in the core state. $\beta_{BM}^{\lambda\lambda'}(y, k_\perp^2)$ is the probability amplitude for the physical nucleon with helicity $+\frac{1}{2}$ in a virtual state consisting of baryon $B^\lambda(y, \vec{k}_\perp)$, with helicity λ, longitudinal momentum y, and transverse momentum $\vec{k}_\perp$, and meson $M^{\lambda'}(1-y, -\vec{k})$, with helicity λ', longitudinal momentum $1-y$, and transverse momentum $-\vec{k}$. $V_{IMF}^{\lambda\lambda'}(y, k_\perp^2)$, is the vertex function, and its explicit form for different baryon-meson pairs with their corresponding helicities are listed in the appendix. The summations in Eq. (14) include all physically possible pairs from the pseudoscalar and vector mesons and their corresponding baryons from the baryon octet and decuplet. Using $\beta_{BM}^{\lambda\lambda'}(y, k_\perp^2)$, one can define polarized splitting function in the following way:

$$n_{BM/N}^\lambda(y) = \sum_{\lambda'}\int_0^\infty dk_\perp^2 |\beta_{BM}^{\lambda\lambda'}(y, k_\perp^2)|^2, \tag{15a}$$

$$n_{MB/N}^{\lambda'}(y) = \sum_{\lambda}\int_0^\infty dk_\perp^2 |\beta_{BM}^{\lambda\lambda'}(1-y, k_\perp^2)|^2. \tag{15b}$$

The splitting functions must satisfy the equations

$$n_{MB}(y) = n_{BM}(1-y), \tag{15c}$$

and

$$\langle x n_{MB}\rangle + \langle x n_{BM}\rangle = \langle n_{BM}\rangle. \tag{15d}$$

In Eq. (15d), $\langle n\rangle$ and $\langle xn\rangle$ are the first and second moments of the splitting functions. Equation (15c) ensures the global charge conservation and Eq. (15d) ensures momentum conservation.

Calculation of the physical polarized quark distributions is basically the same as what was done in Refs. [31,32]. Namely, the polarized core quark distribution can be written as [110]

$$q_{\text{core}}^\lambda(x) = \sum_j \langle N\uparrow|P_{q^\lambda}^j \delta(x - x_j)|N\uparrow\rangle, \tag{16a}$$
$$= 3\langle N\uparrow|P_{q^\lambda}^3 \delta(x - x_3)|N\uparrow\rangle, \tag{16b}$$

with

$$\sum_i x_i = 1, \tag{16c}$$

where $x_1 = \xi\eta$, $x_2 = \eta(1-\xi)$, and $x_3 = 1-\eta$ and $P_{q^\lambda}^j$ is a projection operator that projects out jth quark with helicity λ. Equation (16b) is for the symmetrized wave function. For pseudoscalar and vector meson distributions, we have used the formulation in Refs. [111] and [112], respectively. Using

the core quark distribution along with the meson cloud and their companion baryons, one can obtain the initial quark distributions [31].

These initial distributions are calculated at some initial low Q_0^2. To be able to compare our results with experiments, we evolve these initial distributions using Dokshitzer, Gribov, Lipatov, Altarelli and Parisi (DGLAP) equations [113–115] to some final high Q^2. The DGLAP equations for polarized distributions are [81]

$$\frac{d}{dt}\Delta q_{NS}(x,t) = \frac{\alpha_s(t)}{2\pi}\Delta P_{qq}^{NS}(x) \otimes \Delta q_{NS}(x,t) \quad (17a)$$

for nonsinglet distributions and

$$\frac{d}{dt}\Delta q_S(x,t) = \frac{\alpha_s(t)}{2\pi}\big[\Delta P_{qq}^{S}(x) \otimes \Delta q_S(x,t) + 2n_f \Delta P_{qG}(x) \otimes \Delta G(x,t)\big], \quad (17b)$$

$$\frac{d}{dt}\Delta G(x,t) = \frac{\alpha_s(t)}{2\pi}\big[\Delta P_{Gq}^{S}(x) \otimes \Delta q_S(x,t) + \Delta P_{GG}(x) \otimes \Delta G(x,t)\big] \quad (17c)$$

for singlet distributions. In Eq. (17), α_s is the QCD running coupling constant, Δq and ΔG are the polarized quark and gluon distribution functions, ΔP's are the splitting functions, f is the number of flavors, and t is defined as

$$t = ln\big(Q^2/Q_0^2\big). \quad (17d)$$

With these the polarized distribution functions, one can calculate polarized singlet, a_0, and nonsinglet, a_3 and a_8, distributions as well as g_1^p and g_1^n polarized structure functions along with their first moment in the following way:

$$a_0(x) = \Delta u(x) + \Delta d(x) + \Delta s(x), \quad (18a)$$

$$a_3(x) = \Delta u(x) - \Delta d(x), \quad (18b)$$

$$a_8(x) = \frac{\Delta u(x) + \Delta d(x) - 2\Delta s(x)}{\sqrt{3}}, \quad (18c)$$

$$g_1^p(x) = \frac{1}{2}\left[\frac{4}{9}\Delta u(x) + \frac{1}{9}\Delta d(x) + \frac{1}{9}\Delta s(x)\right], \quad (18d)$$

$$g_1^n(x) = \frac{1}{2}\left[\frac{1}{9}\Delta u(x) + \frac{4}{9}\Delta d(x) + \frac{1}{9}\Delta s(x)\right], \quad (18e)$$

where

$$\Delta q(x) = [q_\uparrow(x) - q_\downarrow(x)] + [\bar{q}_\uparrow(x) - \bar{q}_\downarrow(x)], \quad (18f)$$

and

$$\Gamma_1^p = \int_0^1 g_1^p(x)dx, \quad (19a)$$

$$\Gamma_1^n = \int_0^1 g_1^n(x)dx, \quad (19b)$$

where Eq. (19) represents the first moment of $g_1^p(x)$ and $g_1^n(x)$. Using Eq. (18) and Eq. (19), one can calculate BSR [73,74] and EJSR [75]:

$$S_B = \Gamma_1^p - \Gamma_1^n, \quad (20a)$$

$$S_{\rm EJ}^p = \frac{1}{12}\left(a_3 + \frac{5}{\sqrt{3}}a_8\right), \quad (20b)$$

TABLE I. Parameters used in sets 1, 2, and 3. Here m_u, m_d, β_Q, and β_q are all in GeV, and μ_p and μ_n are in nuclear magneton units. Set 1 represents our diquark-quark model, and set 2 represents parameters used by Schlumpf [105,106].

	m_u	m_d	β_Q	β_q	n_1	n_2	n_3	μ_p	μ_n
Set 1	0.250	0.210	0.25	0.45	2.8	2.8	2.6	2.82	–1.61
Set 2	0.263	0.263	0.607	0.607	3.5	3.5	3.5	2.81	–1.66

$$S_{\rm EJ}^n = \frac{1}{12}\left(-a_3 + \frac{5}{\sqrt{3}}a_8\right). \quad (20c)$$

Using Eqs. (18a)–(18c), one could write polarized quark distributions in terms of singlet and nonsinglet distributions:

$$\Delta u = \frac{(\sqrt{3}a_8 + 2a_0 + 3a_3)}{6}, \quad (21a)$$

$$\Delta d = \frac{(\sqrt{3}a_8 + 2a_0 - 3a_3)}{6}, \quad (21b)$$

$$\Delta s = \frac{(-\sqrt{3}a_8 + a_0)}{3}. \quad (21c)$$

IV. RESULTS AND DISCUSSION

In Table I, we present the parameters, in energy units of GeV, that have been used in Eqs. (12), (13), (16), and (17) to calculate quark distribution functions and the proton and neutron polarized structure functions. Set 1 represents spin-0 diquark distribution for the nucleon core. Set 2 is the parameters used by Schlumpf [105] and represents symmetrical distribution of quarks inside the nucleon. Set 3 is a superposition of spin-0 and spin-1 diquark wave functions.

In Fig. 1, we present polarized xu and xd distributions for the nucleon core. These distributions have been evaluated

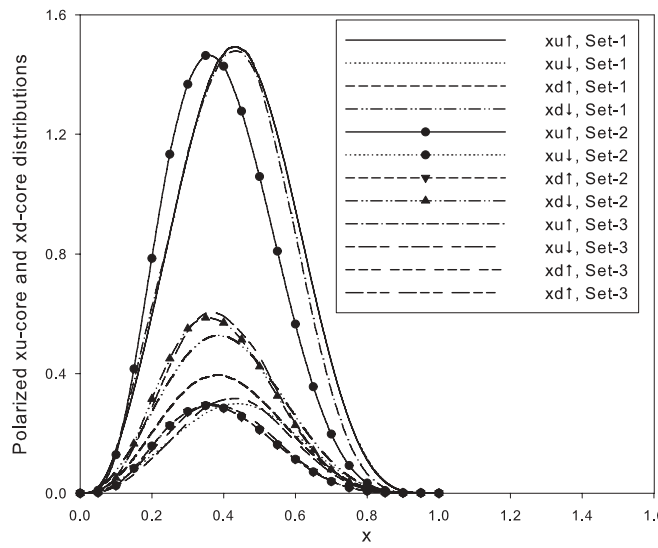

FIG. 1. Polarized xu-core and xd-core distributions for sets 1, 2, and 3. Set 1 represents a spin-0 diquark in a diquark-quark distribution, in set 2 there is no quark clustering, and set 3 represents a superposition of spin-0 and spin-1 diquarks in a diquark-quark distribution.

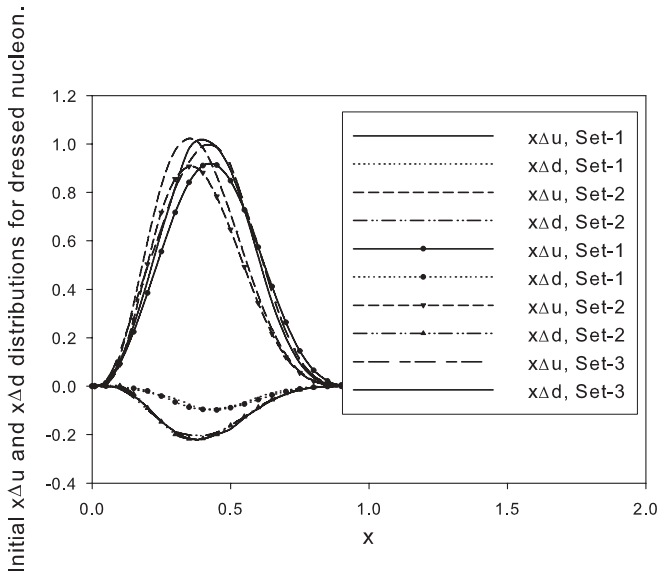

FIG. 2. Initial $x\Delta u$ and $x\Delta d$ distributions for dressed nucleon. The line curves include both vector and pseudoscalar meson contributions, and the line symbol curves include only the pseudoscalar contribution from Ref. [31]. Set 1 represents a spin-0 diquark in a diquark-quark distribution, in set 2 there is no quark clustering, and set 3 represents a superposition of spin-0 and spin-1 diquarks in a diquark-quark distribution.

using Eqs. (16). One can see that the relative closeness of $d_\uparrow$ and $d_\downarrow$ for the spin-0 diquark-quark distribution, which means a rather small magnitude of Δd for set 1. However, for set 3, the gap between $d_\uparrow$ and $d_\downarrow$ is noticeably larger, which leads to a larger d-quark polarization. With these distributions, the bare nucleon is dressed up into a physical nucleon by introducing the meson cloud at some initial low momentum. Figure 2 shows $x\Delta u$ and $x\Delta d$ distributions for sets 1, 2, and 3. In this graph, the line symbol curves include only the pseudoscalar meson cloud, whereas the solid lines include both the pseudoscalar and the vector meson clouds. One can see the noticeable role that the vector meson cloud plays in the quark polarization. Regarding vector mesons, in Ref. [2] we showed that it was the addition of the vector meson cloud that made it possible to reproduce the observed GSR violation. Also, in this graph, one notices that the set 3 Δd is significantly larger than that of set 1 but is comparable with that of set 2. Figure 3 compares s-quark polarization. The first point to be made is that all distributions are positive, in contrast with observation (see, for example, Ref. [56]). However, this is not surprising because we have not introduced any gluon polarization at this stage. At this point, we mention that one can correctly infer that our model does predict asymmetries between the strange and antistrange quark distributions. Also, the vector meson cloud significantly increases the strange quark polarization. However, the overall contribution of the strange quark to nucleon polarization is negligible because the total strangeness in the nucleon is zero. As we have shown in Ref. [2], $\int_0^1 (s(x) + \bar{s}(x))dx = 0$, as it should be. Figures 4, 5, and 6 present the comparisons of xa_3, xa_8, and xa_0 of the present work with those of Ref. [31]. One can see the effect of

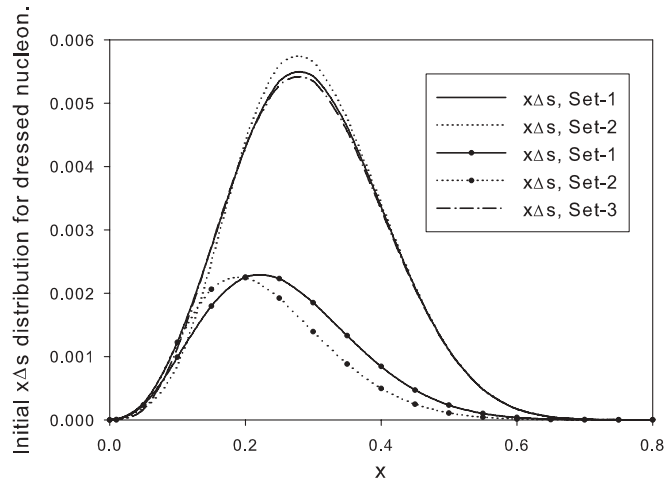

FIG. 3. Initial $x\Delta s$ distributions for the dressed nucleon. The line curves include both vector and pseudoscalar meson contributions, and the line symbol curves include only the pseudoscalar contribution from Ref. [31]. Set 1 represents a spin-0 diquark in a diquark-quark distribution, in set 2 there is no quark clustering, and set 3 represents a superposition of spin-0 and spin-1 diquarks in a diquark-quark distribution.

the dominance of u quark in the quark model. Also, the set 3 results are more comparable with the set 2 results rather than with those of the set 1. These initial distributions are evolved using the code of Kumano and collaborators [116,117] to final momentum transferred and are compared with experimental results. The code uses the modified minimal subtraction ($\overline{MS}$) renormalization scheme and calculates Q^2 evolution to the next-to-leading order of the running coupling constant with QCD scale parameter of 0.2 GeV. To be consistent, we used the same evolution parameter as in Refs. [31] and [32], namely

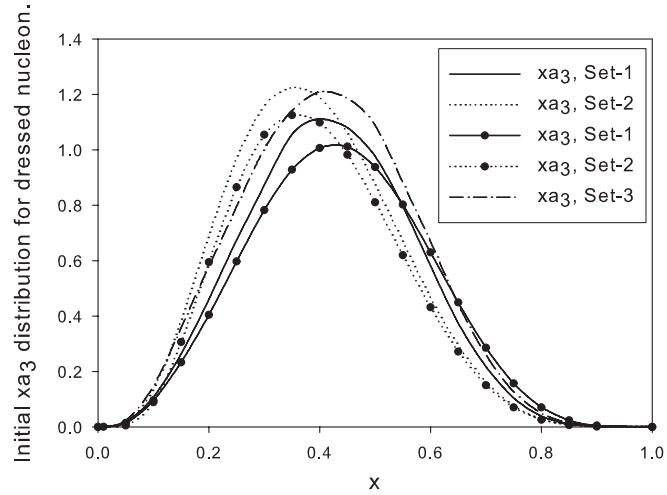

FIG. 4. Initial xa_3 distributions for the dressed nucleon. The line curves include both vector and pseudoscalar meson contributions, and the line symbol curves include only the pseudoscalar contribution from Ref. [31]. Set 1 represents a spin-0 diquark in a diquark-quark distribution, in set 2 there is no quark clustering, and set 3 represents a superposition of spin-0 and spin-1 diquarks in a diquark-quark distribution.

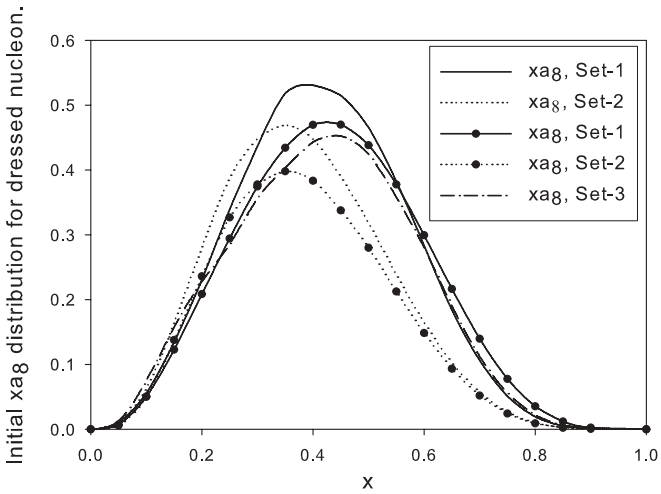

FIG. 5. Initial xa_8 distributions for the dressed nucleon. The line curves include both vector and pseudoscalar meson contributions, and the line symbol curves include only the pseudoscalar contribution from Ref. [31]. Set 1 represents a spin-0 diquark in a diquark-quark distribution, in set 2 there is no quark clustering, and set 3 represents a superposition of spin-0 and spin-1 diquarks in a diquark-quark distribution.

$t' = 0.3$, as defined in Refs. [116,117]. Also, we have assumed that there is no initial gluon polarization. However, evolution generates gluon polarization. In set 1 we get $\Delta G = 0.78$, in set 2 we get $\Delta G = 0.76$, and in set 3 we get $\Delta G = 0.98$. Therefore, set 3 results in an increase of gluon polarization but still less than $\Delta G = 1.21$, which we observed in Ref. [32] when we had not yet introduced the vector meson cloud. Because we are interested in comparing the impact of a variety of nucleon cores and the physical nucleon has a unique gluon polarization, we renormalize total gluon polarization for all

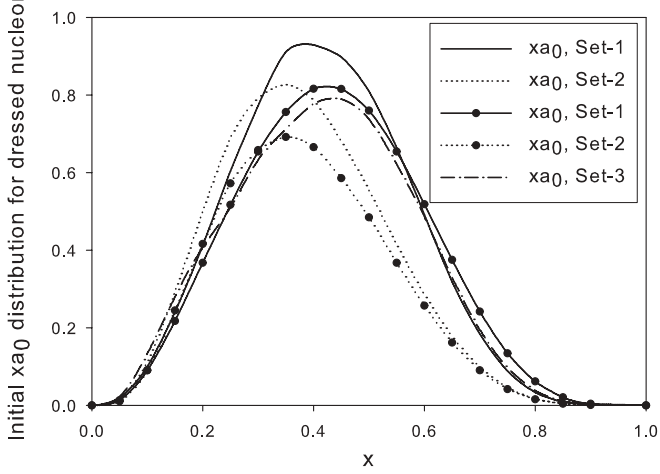

FIG. 6. Initial xa_0 distributions for the dressed nucleon. The line curves include both vector and pseudoscalar meson contributions, and the line symbol curves include only the pseudoscalar contribution from Ref. [31]. Set 1 represents a spin-0 diquark in a diquark-quark distribution, in set 2 there is no quark clustering, and set 3 represents a superposition of spin-0 and spin-1 diquarks in a diquark-quark distribution.

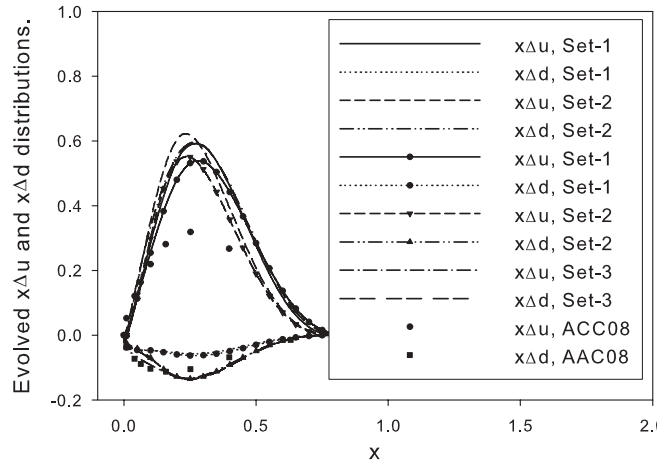

FIG. 7. Evolved $x\Delta u$ and $x\Delta d$ distributions with corrections attributable to gluon anomaly. The line curves include both vector and pseudoscalar meson contributions, and the line symbol curves include only the pseudoscalar contribution from Ref. [31]. The symbols, AAC08, have been generated using calculations by the AAC group Ref. [118]. Set 1 represents a spin-0 diquark in a diquark-quark distribution, in set 2 there is no quark clustering, and set 3 represents a superposition of spin-0 and spin-1 diquarks in a diquark-quark distribution.

sets to be 2.5, the same as in Refs. [31] and [32]. However, to take into account the fact that experimental results favor small gluon polarization, as mentioned in the introduction, we also consider the case of total gluon polarization of 2.0. The initial justification for using a high contribution was that it is not unexpected in pQCD, as explained by Ellis and Karliner [82]. Therefore, one can consider the experimental observation as a superposition of quark and gluon polarization. Taking this into account, one can write

$$\Delta q \longrightarrow \Delta q - \frac{\alpha_s}{2\pi}\Delta G, \tag{22}$$

where α_s is QCD running coupling constant. In our case, we chose $\frac{\alpha_s}{2\pi} = 0.048$, which means Q^2 is about 4 GeV^2. Therefore, we are fitting our data to a final scale of 4 GeV^2. Knowing the evolution parameter fixes our initial model scale at $Q_0 = 0.390$ GeV, which is in line with that of Ref. [15].

The results that take into account Eq. (22) for evolved distributions are shown in Figs. 7–11. To avoid overcrowding the graphs, instead of comparing our work with data from several experiments, we compare our work with the best fit to world experimental data by the AAC group [118]. As expected, the evolution results in the shift of the distribution peaks to lower x. In Fig. 7, d-quark polarizations for sets 2 and 3 are very close to each other and are in better agreement with AAC than set 1, which predicts a very small d-quark polarization. Also, the inclusion of a gluon anomaly leads to a reasonable agreement of polarized strange quark distributon with observation, as can be seen in Fig. 8. Because the addition of the vector mesons leads to an increase in u-quark polarization, one can see from Figs. 7 and 9–11 that set 2 leads to the best agreement with experimental data for $x\Delta u$, xa_3, xa_8, and xa_0, respectively. As shown in Ref. [31], introduction

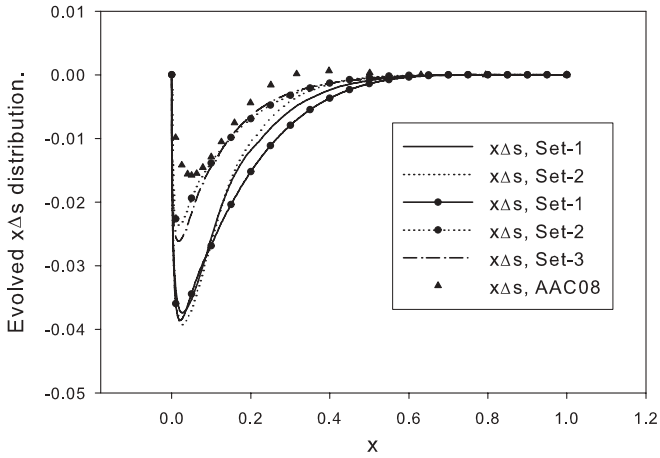

FIG. 8. Evolved $x\Delta s$ distributions with corrections attributable to gluon anomaly. The line curves include both vector and pseudoscalar meson contributions, and the line symbol curves include only the pseudoscalar contribution from Ref. [31]. The symbols, AAC08, have been generated using calculations by the AAC group Ref. [118]. Set 1 represents a spin-0 diquark in a diquark-quark distribution, in set 2 there is no quark clustering, and set 3 represents a superposition of spin-0 and spin-1 diquarks in a diquark-quark distribution.

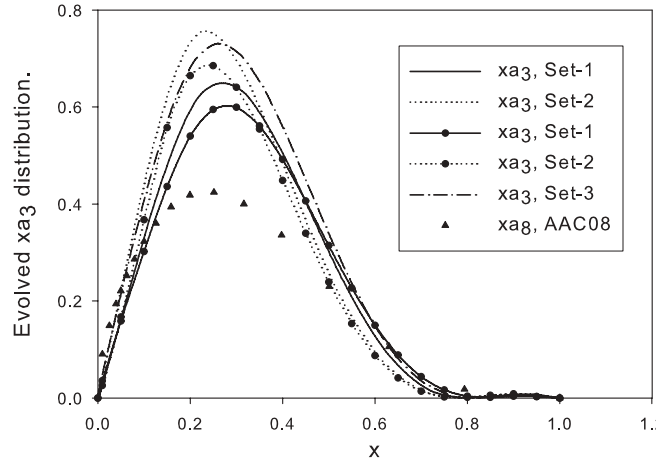

FIG. 9. Evolved xa_3 distributions with corrections attributable to gluon anomaly. The line curves include both vector and pseudoscalar meson contributions, and the line symbol curves include only the pseudoscalar contribution from Ref. [31]. The symbols, AAC08, have been generated using calculations by the AAC group Ref. [118]. Set 1 represents a spin-0 diquark in a diquark-quark distribution, in set 2 there is no quark clustering, and set 3 represents a superposition of spin-0 and spin-1 diquarks in a diquark-quark distribution.

of vector mesons did not lead to a better agreement of set 1 with observations for xa_3, xa_8, and xa_0. However, set 3, which includes vector mesons, is in better agreement with observations than set 1 with only pseudoscalar mesons for xa_8 and xa_0. For Δd and Δs, one can see from Figs. 7 and 8, respectively, that the addition of the vector mesons leads to better agreement with observations. Our numerical results along with some experimental and theoretical results are presented in Table II. There are few points to be made concerning these data. Comparing sets 3 and 1, one can see that set 3 generates a large magnitude of Δd and negative first moment of g_1^n, which is in agreement with observations [48,55,56,66]. Set 1, even after addition of vector mesons and introduction of gluon anomaly, results in small magnitude of Δd and positive first moment of g_1^n, which is in contrast with observations [48,55,56,66]. Both sets reproduce strange quark polarizations nicely, but set 1 is in better agreement with BSR than set 3. Set 2 results are more in line with those of set 3. With the exception of set 1 of Ref. [32], which is in agreement with the HERMES (NNNLO) BSR calculation, our model

TABLE II. Comparison of the results of our models with theory and experiment. The first four rows are experimental results corresponding to Refs. [57], [56], [49], and [66] respectively. The fifth row corresponds to Ellis-Jaffe [75] and Bjorken [73,74] sum rules. The sixth and seventh rows are leading-order and next-to-next-to-next-leading-order calculations [66]. Row 8 is simply the nonrelativistic quark parton model prediction. The ninth row corresponds to relativistic quark model calculations [121]. The results of our work are presented in the last six rows.

	Δu	Δd	Δs	Γ_1^p	Γ_1^n	$\Gamma_1^p - \Gamma_1^n$
E143 (3 GeV^2)	0.83	−0.43	−0.09	0.133	−0.032	0.165
E154 (5 GeV^2)				0.122	−0.056	0.168
SMC (5 GeV^2)				0.132	−0.048	0.181
HERMES (5 GeV^2)	0.842	−0.427	−0.085	0.121	−.027	0.148
EJSR/BSR				0.167	−0.015	0.182
HERMES (5 GeV^2 LO)				0.153	−0.059	0.212
HERMES (5 GeV^2 NNNLO)				0.138	−0.044	0.182
NRQPM ($\Delta G = 0$)	1.33	−0.33	0			
RQPM ($\Delta G = 0$)	1.0	−0.25	0			
Set 1 ($\Delta G = 2.50$, Ref. [32])	0.917	−0.195	−0.105	0.187	0.002	0.185
Set 2 ($\Delta G = 2.50$, Ref. [32])	0.951	−0.271	−0.059	0.193	−0.011	0.204
Set 1 ($\Delta G = 2.50$, Ref. [31])	1.00	−0.187	−0.100	0.208	0.009	0.199
Set 2 ($\Delta G = 2.50$, Ref. [31])	1.07	−0.324	−0.101	0.213	−0.018	0.231
Set 3 ($\Delta G = 2.50$, current work)	1.10	−0.326	−0.105	0.221	−0.017	0.238
Set 3 ($\Delta G = 2.00$, current work)	1.13	−0.302	−0.081	0.229	−0.009	0.238

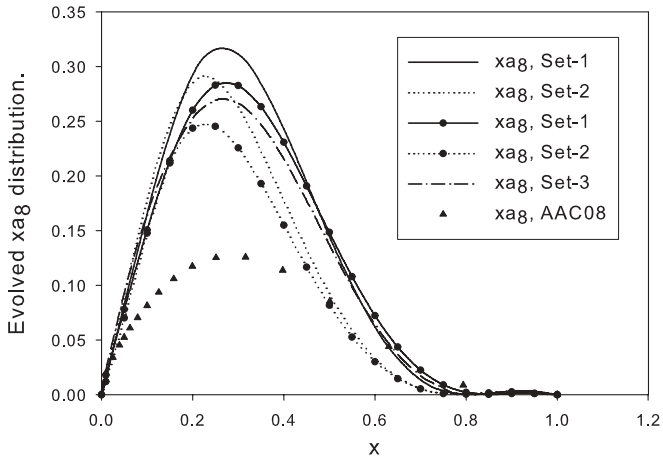

FIG. 10. Evolved xa_8 distributions with corrections attributable to gluon anomaly. The line curves include both vector and pseudoscalar meson contributions, whereas the line symbol curves include only the pseudoscalar contribution from Ref. [31]. The symbols, AAC08, have been generated using calculations by the AAC group Ref. [118]. Set 1 represents a spin-0 diquark in a diquark-quark distribution, in set 2 there is no quark clustering, and set 3 represents a superposition of spin-0 and spin-1 diquarks in a diquark-quark distribution.

calculations are more in line with the HERMES (LO) BSR calculations, where LO indicates the leading order term and NNNLO indicates the leading order term plus the next three terms of the perturbation series. Comparing the last six rows of Table II with the theoretical calculations for non-relativistic quark-parton model (NRQPM) row and relativistic quark-parton model (RQPM) row, one realizes that the introduction

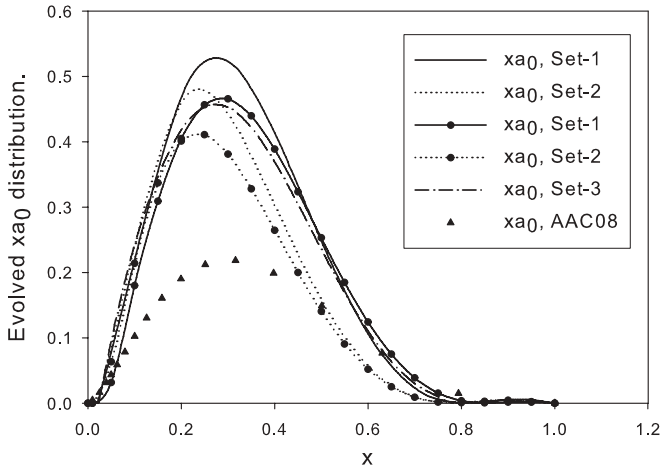

FIG. 11. Evolved xa_0 distributions with corrections attributable to gluon anomaly. The line curves include both vector and pseudoscalar meson contributions, and the line symbol curves include only the pseudoscalar contribution from Ref. [31]. The symbols, AAC08, have been generated using calculations by the AAC group Ref. [118]. Set 1 represents a spin-0 diquark in a diquark-quark distribution, in set 2 there is no quark clustering, and set 3 represents a superposition of spin-0 and spin-1 diquarks in a diquark-quark distribution.

of the meson cloud in the relativistic quark model results in better agreement with experimental results, which once again shows the significance of the role of the meson cloud in nucleon structure.

V. SUMMARY

Over a series of calculations, we have used three different nucleon core distributions, namely, the no diquark model, the spin-0 diquark model, and the superposition of spin-0 and spin-1 diquarks model, in a relativistic quark model along with pseudoscalar mesons and vector mesons to evaluate polarized and unpolarized nucleon structure functions. Our results show that the no diquark model fails to reproduce the F_2 structure function, which is in agreement with experimental results for moderate to high x values. However, the model is reasonably successful in evaluation of the g_1 structure function for the nucleon and the BSR when one includes both classes of meson cloud. The spin-0 diquark does a much better job in F_2 calculations but underestimates the GSR violation. However, this model fails to agree with experimental results for the polarized case. For example, it predicts positive first moment of the g_1 structure function for the neutron. The third model, namely, a superposition of spin-0 and spin-1 diquarks, is the only model that was reasonably successful in evaluation of both F_2 and g_1 structure functions. Also, it is the only model that reproduces the experimental observations for GSR violations when one includes both the pseudoscalar mesons and the vector mesons.

APPENDIX

The explicit form of the vertex function, $V^{\lambda\lambda'}_{IMF}(y, k^2_\perp)$, used in Eq. (14b) is

$$V^{\lambda\lambda'}_{IMF}(y, k^2_\perp) = \left|\Gamma_{MB}\left(M^2_{MB}\right)\right|^2 V'^{\lambda\lambda'}_{IMF}(y, k^2_\perp), \tag{A1}$$

where $\Gamma_{MB}(M^2_{MB})$ is the vertex form factor and is parameterized by the exponential function of the invariant mass, M_{MB}, of the intermediate baryon-meson state:

$$\Gamma_{MB}\left(M^2_{MB}\right) = e^{-(M^2_{MB}-m^2_N)/\Lambda^2_{MB}}, \tag{A2}$$

where λ_{MB} are free parameters determined by fitting experimental data. In the following, we present the explicit form of $V'^{\lambda\lambda'}_{IMF}(y, k^2_\perp)$, for intermediate helicity states of pseudoscalar meson and baryon states, calculated by Holtmann and collaborators [36,37].For intermediate states $N\pi$, $N\eta$, ΣK, and ΛK, the vertex functions are

$$\frac{1}{2} \to +\frac{1}{2}, \quad 0 \quad \frac{g_{NMB}}{2}\frac{ym_N - m_B}{\sqrt{ym_N m_B}}, \tag{A3}$$

$$\frac{1}{2} \to -\frac{1}{2}, \quad 0 \quad \frac{g_{NMB}e^{-i\phi}}{2}\frac{k_\perp}{\sqrt{ym_N m_B}}. \tag{A4}$$

For $\Delta\pi$, $\Sigma^* K$ intermediate states, we have

$$\frac{1}{2} \to +\frac{3}{2}, \quad 0 \quad -\frac{f_{NMB}e^{+i\phi}}{2\sqrt{2}}\frac{k_\perp(ym_N + m_B)}{y\sqrt{ym_N m_B}}, \tag{A5}$$

$$\frac{1}{2} \to +\frac{1}{2}, \quad 0 \quad \frac{f_{NMB}}{2\sqrt{6}} \frac{(ym_N + m_B)^2(ym_N - m_B) + k_\perp^2(ym_N + 2m_B)}{ym_B\sqrt{ym_N m_B}}, \tag{A6}$$

$$\frac{1}{2} \to -\frac{1}{2}, \quad 0 \quad \frac{f_{NMB}e^{-i\phi}}{2\sqrt{6}} \frac{k_\perp[(ym_N + m_B)^2 - 3m_B(ym_N + 2m_B) + k_\perp^2]}{ym_B\sqrt{ym_N m_B}}, \tag{A7}$$

$$\frac{1}{2} \to -\frac{3}{2}, \quad 0 \quad -\frac{f_{NMB}e^{-2i\phi}}{2\sqrt{2}} \frac{k_\perp^2}{y\sqrt{ym_N m_B}}. \tag{A8}$$

For $N\rho$, $N\omega$, ΣK^*, and ΛK^* intermediate states, we have

$$\frac{1}{2} \to +\frac{1}{2}, \quad +1 \quad \frac{g_{NMB}e^{+i\phi}}{\sqrt{2}} \frac{k_\perp}{(1-y)\sqrt{ym_N m_B}} - f_{NMB}\sqrt{2}e^{+i\phi} \frac{k_\perp m_N}{\sqrt{ym_N m_B}}, \tag{A9}$$

$$\frac{1}{2} \to +\frac{1}{2}, \quad 0 \quad \frac{g_{NMB}}{2} \frac{k_\perp^2 + m_N m_B(1-y)^2 - ym_M^2}{2(1-y)m_M\sqrt{ym_N m_B}} - \frac{f_{NMB}}{2} \frac{(ym_N - m_B)\left[y^2 m_N^2 - y\left(m_N^2 + m_B^2 + m_M^2\right) + m_B^2 + k_\perp^2\right]}{ym_M\sqrt{ym_N m_B}}, \tag{A10}$$

$$\frac{1}{2} \to +\frac{1}{2}, \quad -1 \quad \frac{g_{NMB}e^{-i\phi}}{\sqrt{2}} \frac{yk_\perp}{(1-y)\sqrt{ym_N m_B}} + f_{NMB}\sqrt{2}e^{-i\phi} \frac{k_\perp m_B}{\sqrt{ym_N m_B}}, \tag{A11}$$

$$\frac{1}{2} \to -\frac{1}{2}, \quad +1 \quad \frac{g_{NMB}}{\sqrt{2}} \frac{ym_N - m_B}{\sqrt{ym_N m_B}} - f_{NMB}\sqrt{2} \frac{k_\perp^2 - (m_N + m_B)(1-y)(ym_N - m_B)}{(1-y)\sqrt{ym_N m_B}}, \tag{A12}$$

$$\frac{1}{2} \to -\frac{1}{2}, \quad 0 \quad -\frac{g_{NMB}e^{-i\phi}}{2} \frac{k_\perp + (m_N - m_B)}{m_M\sqrt{ym_N m_B}} - \frac{f_{NMB}e^{-i\phi}}{2} \frac{k_\perp(1+y)\left[y^2 m_N^2 - y\left(m_N^2 + m_B^2 + m_M^2\right) + m_B^2 + k_\perp^2\right]}{y(1-y)m_M\sqrt{ym_N m_B}}, \tag{A13}$$

$$\frac{1}{2} \to +\frac{1}{2}, \quad -1 \quad f_{NMB}\sqrt{2}e^{-2i\phi} \frac{k_\perp^2}{(1-y)\sqrt{ym_N m_B}}. \tag{A14}$$

$$\frac{1}{2} \to +\frac{1}{2}, \quad +1 \quad \frac{f_{NMB}e^{+i\phi}}{2\sqrt{3}} \frac{k_\perp\left[k_\perp^2 - 2(1-y)m_B^2\right]}{y(1-y)m_B\sqrt{ym_N m_B}}, \tag{A18}$$

Finally, for $\Delta\rho$, $\Sigma^* K^*$, we have

$$\frac{1}{2} \to +\frac{3}{2}, \quad +1 \quad -\frac{f_{NMB}e^{+2i\phi}}{2} \frac{k_\perp}{y(1-y)\sqrt{ym_N m_B}}, \tag{A15}$$

$$\frac{1}{2} \to +\frac{3}{2}, \quad 0 \quad \frac{f_{NMB}e^{+i\phi}}{\sqrt{2}} \frac{k_\perp m_N}{(1-y)\sqrt{ym_N m_B}}, \tag{A16}$$

$$\frac{1}{2} \to +\frac{3}{2}, \quad -1 \quad \frac{f_{NMB}}{2} \frac{m_N m_B(1-y)^2 - ym_M^2}{(1-y)\sqrt{ym_N m_B}}, \tag{A17}$$

$$\frac{1}{2} \to +\frac{1}{2}, \quad 0 \quad -\frac{f_{NMB}}{\sqrt{6}} \frac{m_M[k_\perp^2 + m_B(1-y)(ym_N - m_B)]}{(1-y)m_B\sqrt{ym_N m_B}}, \tag{A19}$$

$$\frac{1}{2} \to +\frac{1}{2}, \quad -1 \quad \frac{f_{NMB}e^{-i\phi}}{2\sqrt{3}} \frac{k_\perp[ym_M^2 - 2m_N m_B(1-y)]}{(1-y)m_B\sqrt{ym_N m_B}}, \tag{A20}$$

$$\frac{1}{2} \to -\frac{1}{2}, \quad +1 \quad \frac{f_{NMB}e^{-i\phi}}{2\sqrt{3}} \frac{2(1-y)m_B k_\perp^2 + m_N m_M^2 y^3 - (1-y)^2 m_B^3}{y(1-y)m_B\sqrt{ym_N m_B}}, \tag{A21}$$

$$\frac{1}{2} \to -\frac{1}{2}, \quad 0 \quad \frac{f_{NMB}e^{-i\phi}}{\sqrt{6}} \frac{k_\perp m_M(ym_N - (1-y)m_B)}{(1-y)m_B\sqrt{ym_N m_B}}, \tag{A22}$$

$$\frac{1}{2} \to -\frac{1}{2}, \quad -1 \quad \frac{f_{NMB}e^{-2i\phi}}{2\sqrt{3}} \frac{k_\perp^2 m_N}{(1-y)m_B\sqrt{ym_N m_B}}, \tag{A23}$$

$$\frac{1}{2} \to -\frac{3}{2}, \quad +1 \quad \frac{f_{NMB}e^{-i\phi}}{2} \frac{k_\perp m_B(1-y)}{y\sqrt{ym_N m_B}}, \tag{A24}$$

$$\frac{1}{2} \to -\frac{3}{2}, \quad 0 \quad 0, \tag{A25}$$

$$\frac{1}{2} \to -\frac{3}{2}, \quad -1 \quad 0. \tag{A26}$$

In these equations, we have used the notation $1/2 \to \lambda, \lambda'$, where λ and λ' are the helicities of the baryon and meson respectively, y is the longitudinal momentum fraction of the baryon, and ϕ is the angle between the baryon's transverse momentum and that of the nucleon; g_{NMB} and f_{NMB} are the coupling constants, which we choose [14,36,119] to be $\frac{g^2_{p\pi^0 p}}{4\pi} = 13.6$, $\frac{g^2_{p\rho^0 p}}{4\pi} = 0.84$, $\frac{g^2_{p\omega p}}{4\pi} = 8.1$, $\frac{f^2_{p\pi^- \Delta^{++}}}{4\pi} = 10.85\ \text{GeV}^{-2}$, $\frac{f^2_{p\rho^- \Delta^{++}}}{4\pi} = 34.7\ \text{GeV}^{-2}$, $\frac{f^2_{pp^0 p}}{4\pi} = 31.25\ \text{GeV}^{-2}$, and $\frac{f^2_{p\omega p}}{4\pi} = 0$.Other coupling constants are related to these two through the quark model [36,119,120].

[1] J. D. Sullivan, Phys. Rev. D **5**, 1732 (1972).
[2] F. Zamani, Phys. Rev. C **79**, 035208 (2009).
[3] F. Zamani, Phys. Rev. C **74**, 035204 (2006).
[4] F. Zamani, Nucl. Phys. A **755**, 365 (2005).
[5] F. Zamani, Phys. Rev. C **58**, 3641 (1998).
[6] A. W. Thomas, Nucl. Phys. A **518**, 186 (1990).
[7] S. Kumano, Phys. Rev. D **41**, 195 (1990).
[8] A. W. Thomas and G. A. Miller, Phys. Rev. D **43**, 288 (1991).
[9] W. Y. P. Hwang, J. Speth, and G. E. Brown, Z. Phys. A **339**, 383 (1991).
[10] S. Kumano, Phys. Rev. D **43**, 59 (1991).
[11] S. Kumano, Phys. Rev. D **43**, 3067 (1991).
[12] S. Kumano and J. T. Londergan, Phys. Rev. D **44**, 717 (1991).
[13] W. Melnitchouk, A. W. Thomas, and A. I. Signal, Z. Phys. A **340**, 85 (1991).
[14] V. R. Zoller, Z. Phys. C **53**, 443 (1992).
[15] A. W. Schreiber, P. J. Mulders, A. I. Signal, and A. W. Thomas, Phys. Rev. D **45**, 3069 (1992).
[16] W. Y. P. Hwang and J. Speth, Phys. Rev. D **46**, 1198 (1992).
[17] A. W. Thomas and W. Melnitchouk, *New Frontiers in Nuclear Physics* (World Scientific, Singapore, 1993), p. 41.
[18] A. Szczurek and J. Speth, Nucl. Phys. A **555**, 249 (1993).
[19] A. Szczurek, J. Speth, and G. T. Garvey, Nucl. Phys. A **570**, 765 (1994).
[20] N. N. Nikolaev, A. Szczurek, J. Speth, and V. R. Zoller, Z. Phys. A **349**, 59 (1994).
[21] B. C. Pearce, J. Speth, and A. Szczurek, Phys. Rep. **242**, 193 (1994).
[22] A. Szczurek, M. Ericson, H. Holtmann, and J. Speth, Nucl. Phys. A **596**, 397 (1996).
[23] A. Szczurek, A. J. Buchmann, and A. Faessler, J. Phys. G **22**, 1741 (1996).
[24] S. J. Brodsky and B.-Q. Ma, Phys. Lett. B **381**, 317 (1996).
[25] W. Koepf, L. L. Frankfurt, and M. Strikman, Phys. Rev. D **53**, 2586 (1996).
[26] F. M. Steffens and A. W. Thomas, Phys. Rev. C **55**, 900 (1997).
[27] S. D. Bass and D. Schutte, Z. Phys. A **357**, 85 (1997).
[28] S. Kumano, Phys. Rep. **303**, 183 (1998).
[29] F. S. Navarra, M. Nielsen, and S. Paiva, Phys. Rev. D **56**, 3041 (1997).
[30] S. Paiva, M. Neilson, F. S. Navarra, F. O. Duraes, and L. L. Barz, Mod. Phys. Lett. A **13**, 2715 (1998).
[31] F. Zamani, Phys. Rev. C **68**, 055202 (2003).
[32] F. Zamani and D. Saranchak, Phys. Rev. C **63**, 065202 (2001).
[33] V. R. Zoller, Mod. Phys. Lett. A **8**, 1113 (1993).
[34] F. M. Steffens, H. Holtmann, and A. W. Thomas, Phys. Lett. B **358**, 139 (1995).
[35] W. Melnitchouk and A. W. Thomas, Z. Phys. A **353**, 311 (1995).
[36] H. Holtmann, A. Szczurek, and J. Speth, Nucl. Phys. A **596**, 631 (1996).
[37] J. Speth and A. W. Thomas, Adv. Nucl. Phys. **24**, 83 (1997).
[38] K. G. Boreskov, A. B. Kaidalov, Y. B. Dong, K. Shimizu, A. Faessler, and A. J. Buchmann, J. Phys. G **25**, 1115 (1999).
[39] S. Kumano and M. Miyama, Phys. Rev. D **65**, 034012 (2002).
[40] J. Ashman *et al.*, Phys. Lett. B **206**, 364 (1988).
[41] J. Ashman *et al.*, Nucl. Phys. B **328**, 1 (1989).
[42] B. Adeva *et al.*, Phys. Lett. B **302**, 533 (1993).
[43] D. Adams *et al.*, Phys. Lett. B **329**, 399 (1994).
[44] D. Adams *et al.*, Phys. Lett. B **357**, 248 (1995).
[45] D. Adams *et al.*, Phys. Lett. B **396**, 338 (1997).
[46] D. Adams *et al.*, Phys. Rev. D **56**, 5330 (1997).
[47] B. Adeva *et al.*, Phys. Lett. B **412**, 414 (1997).
[48] B. Adeva *et al.*, Phys. Rev. D **58**, 112001 (1998).
[49] B. Adeva *et al.*, Phys. Rev. D **60**, 072004 (1999).
[50] J. Le Goff *et al.*, Nucl. Phys. A **666**, 296 (2000).
[51] P. L. Anthony *et al.*, Phys. Rev. Lett. **71**, 959 (1993).
[52] P. L. Anthony *et al.*, Phys. Rev. D **54**, 6620 (1996).
[53] K. Abe *et al.*, Phys. Rev. Lett. **74**, 346 (1995).
[54] K. Abe *et al.*, Phys. Rev. Lett. **75**, 25 (1995).
[55] K. Abe *et al.*, Phys. Lett. B **364**, 61 (1995).
[56] K. Abe *et al.*, Phys. Rev. Lett. **79**, 26 (1997).
[57] K. Abe *et al.*, Phys. Rev. D **58**, 112003 (1998).
[58] P. L. Anthony *et al.*, Phys. Lett. B **463**, 339 (1999).
[59] O. Rondon, Nucl. Phys. A **663**, 293 (1997).
[60] P. L. Anthony *et al.*, Phys. Lett. B **493**, 19 (2000).
[61] K. Ackerstaff *et al.*, Phys. Lett. B **404**, 383 (1997).
[62] A. Airapetian *et al.*, Phys. Lett. B **442**, 484 (1998).
[63] A. Simon *et al.*, Nucl. Phys. Proc. Suppl. **86**, 112 (2000).
[64] A. Brull *et al.*, Nucl. Phys. A **663**, 317 (2000).
[65] A. Airapetian *et al.*, Phys. Rev. D **71**, 012003 (2005).
[66] A. Airapetian *et al.*, Phys. Rev. D **75**, 012007 (2007).
[67] M. Amarian *et al.*, Phys. Rev. Lett. **92**, 022301 (2004).
[68] A. Deur *et al.*, Phys. Rev. Lett. **93**, 212001 (2004).
[69] X. Zheng *et al.*, Phys. Rev. Lett. **92**, 012004 (2004).
[70] X. Zheng *et al.*, Phys. Rev. C **70**, 065207 (2004).
[71] J. P. Chen, A. Deur, and Z. E. Meziani, Mod. Phys. Lett. A **20**, 2745 (2005).
[72] K. Kramer *et al.*, Phys. Rev. Lett. **95**, 142002 (2005).
[73] J. D. Bjorken, Phys. Rev. **148**, 1467 (1966).
[74] J. D. Bjorken, Phys. Rev. D **1**, 1376 (1970).
[75] J. Ellis and R. Jaffe, Phys. Rev. D **9**, 1444 (1974).
[76] G. Altarelli and G. G. Ross, Phys. Lett. B **212**, 391 (1988).
[77] R. D. Carlitz, J. C. Collins, and A. H. Mueller, Phys. Lett. B **214**, 229 (1988).
[78] A. V. Efremov, J. Soffer, and O. V. Teryaev, Nucl. Phys. B **346**, 97 (1990).
[79] G. T. Bodwin and J. Qiu, Phys. Rev. D **41**, 2755 (1990).
[80] S. D. Bass and A. W. Thomas, J. Phys. G **19**, 925 (1993).
[81] H. Y. Cheng, Chin. J. Phys. **38**, 753 (2000).
[82] J. Ellis and M. Karliner, arXiv:hep-ph/9601280.
[83] J. Ellis and M. Karliner, Mod. Phys. Lett. A **21**, 721 (2006).
[84] E. S. Ageev *et al.*, Phys. Lett. B **633**, 25 (2006).
[85] D. Kotlorz and A. Kotlorz, Acta Phys. Polon. B **39**, 1913 (2008).
[86] S. E. Kuhn, J. P. Chen, and E. Leader, Prog. Part. Nucl. Phys. **63**, 1 (2009).
[87] R. L. Jaffe and A. Manohar, Nucl. Phys. B **337**, 509 (1990).
[88] M. Anselmino, A. Efremov, and E. Leader, Phys. Rep. **261**, 1 (1995).
[89] V. U. Stiegler, Phys. Rep. **277**, 1 (1996).
[90] I. Hinchliffe and A. Kwiatkowski, Annu. Rev. Nucl. Part. Sci. **46**, 609 (1996).
[91] G. P. Ramsey, Prog. Part. Nucl. Phys. **39**, 599 (1997).
[92] L. F. Li and T. P. Cheng, arXiv:hep-ph/9709293.
[93] G. Altarelli, R. D. Ball, S. Forte, and G. Ridolfi, Acta Phys. Polon. B **29**, 1145 (1998).
[94] M. C. Vetterli, arXiv:hep-ph/9812420.
[95] J. Kodaira and K. Tanaka, Prog. Theor. Phys. **101**, 191 (1999).
[96] B. Lampe and E. Reya, Phys. Rep. **332**, 1 (2000).
[97] P. J. Mulders, Prog. Part. Nucl. Phys. **55**, 243 (2005).
[98] F. Bissey, F.-G. Cao, and A. I. Signal, Phys. Rev. D **73**, 094008 (2006).
[99] W. Vogelsang, J. Phys. G **34**, S149 (2007)

[100] P. A. M. Dirac, Rev. Mod. Phys. **21**, 392 (1949).
[101] H. Leutwyler and J. Stern, Ann. Phys. **112**, 94 (1978).
[102] M. G. Fuda, Ann. Phys. **197**, 265 (1990).
[103] M. G. Fuda, Ann. Phys. **231**, 1 (1994).
[104] M. Burkardt, Adv. Nucl. Phys. **23**, 1 (1996).
[105] F. Schlumpf, Ph.D. thesis, University of Zurich, 1992.
[106] F. Schlumpf, Phys. Rev. D **47**, 4114 (1993).
[107] V. B. Berestetskii and M. V. Terent'ev, Sov. J. Nucl. Phys. **24**, 547 (1976).
[108] V. B. Berestetskii and M. V. Terent'ev, Sov. J. Nucl. Phys. **25**, 347 (1977).
[109] H. J. Melosh, Phys. Rev. D **9**, 1095 (1974).
[110] Z. Dziembowski, C. J. Martoff, and P. Zyla, Phys. Rev. D **50**, 5613 (1994).
[111] C. M. Shakin and W.-D. Sun, Phys. Rev. C **53**, 3152 (1996).
[112] H. M. Choi, Ph.D. thesis, North Carolina State University, 1999.
[113] V. N. Gribov and L. N. Lipatov, Sov. J. Nucl. Phys. **15**, 675 (1972).
[114] G. Altarelli and G. Parisi, Nucl. Phys. B **126**, 298 (1977).
[115] Y. L. Dokshitzer, Sov. Phys. JETP **46**, 641 (1977).
[116] S. Kumano and J. T. Londergan, Comput. Phys. Commun. **69**, 373 (1992).
[117] R. Kobayashi, M. Konuma, and S. Kumano, Comput. Phys. Commun. **86**, 264 (1995).
[118] [http://spin.riken.bnl.gov/aac/].
[119] B. Holzenkamp, K. Holinde, and J. Speth, Nucl. Phys. A **500**, 485 (1989).
[120] G. E. Brown and W. Weise, Phys. Rep. C **22**, 279 (1975).
[121] S. J. Brodsky and F. Schlumpf, Phys. Lett. B **329**, 111 (1994).